

Structure-Based Design, Synthesis, and Biological Evaluation of Imidazo[4,5-*b*]Pyridin-2-one-Based p38 MAP Kinase Inhibitors: Part 2

Akira Kaieda,^{*,[a]} Masashi Takahashi,^[a] Hiromi Fukuda,^[a] Rei Okamoto,^[a] Shinji Morimoto,^[a] Masayuki Gotoh,^[a] Takahiro Miyazaki,^[a] Yuri Hori,^[a] Satoko Unno,^[a] Tomohiro Kawamoto,^[a] Toshimasa Tanaka,^[a] Sachiko Itono,^[a] Terufumi Takagi,^[a] Hiroshi Sugimoto,^[a] Kengo Okada,^[a] Weston Lane,^[b] Bi-Ching Sang,^[b] Kumar Saikatendu,^[b] Shinichiro Matsunaga,^[a] and Seiji Miwatashi^[a]

We identified novel potent inhibitors of p38 mitogen-activated protein (MAP) kinase using a structure-based design strategy, beginning with lead compound, 3-(butan-2-yl)-6-(2,4-difluoroanilino)-1,3-dihydro-2*H*-imidazo[4,5-*b*]pyridin-2-one (**1**). To enhance the inhibitory activity of **1** against production of tumor necrosis factor- α (TNF- α) in human whole blood (hWB) cell assays, we designed and synthesized hybrid compounds in which the imidazo[4,5-*b*]pyridin-2-one core was successfully linked with the *p*-methylbenzamide fragment. Among the

compounds evaluated, 3-(3-*tert*-butyl-2-oxo-2,3-dihydro-1*H*-imidazo[4,5-*b*]pyridin-6-yl)-4-methyl-*N*-(1-methyl-1*H*-pyrazol-3-yl) benzamide (**25**) exhibited potent p38 inhibition, superior suppression of TNF- α production in hWB cells, and also significant *in vivo* efficacy in a rat model of collagen-induced arthritis (CIA). In this paper, we report the discovery of potent, selective, and orally bioavailable imidazo[4,5-*b*]pyridin-2-one-based p38 MAP kinase inhibitors.

Introduction

The p38 α mitogen-activated protein (MAP) kinase is widely expressed in endothelial, immune, and inflammatory cells, and plays a critical role in regulating the biosynthesis of proinflammatory cytokines.^[1,2] Selective biological agents targeting these proinflammatory cytokines have been proven to be efficacious in the treatment of inflammatory diseases, including rheumatoid arthritis (RA), psoriasis, and inflammatory bowel disease.^[3,4] Anti-tumor necrosis factor- α (TNF- α) monoclonal antibodies, including infliximab^[5-7] and adalimumab,^[8,9] and the TNF- α receptor fusion protein, etanercept,^[10] are currently being used as effective anti-RA agents, and have shown good efficacy in patients with active RA.

The MAP kinase family includes the extracellular signal-regulated kinases, c-JUN N-terminal kinases, and p38 MAP kinases. Analyses of MAP kinases from the synovial tissues and cells of patients with RA indicated that the p38 α isoform is

overactive in the inflammatory tissues.^[11-13] Therefore, the development of p38 MAP kinase inhibitors has been considered to be a promising solution for the treatment of RA.^[14-18]

Numerous preclinical studies have reported that the inhibition of p38 MAP kinase effectively suppresses the production of TNF- α both *in vitro* and *in vivo*.^[19] Multiple chemical classes of p38 MAP kinase inhibitors have been discovered, including VX-745,^[20] BCT-197, LY-2228820, GW856553,^[21,22] PH-797804, AZD-7624, CHF-6297, FX-005, and ARRY-797, which have been examined in phase II clinical trials, and are represented in Figure 1.^[23] Another approach for suppression of the production of TNF- α has reported, CBS-3595 in phase I has been discovered as a dual inhibitor of p38 MAP kinase and phosphodiesterase 4.^[24]

We have previously reported the design and synthesis of p38 MAP kinase inhibitors derived from 1,3-thiazole^[16] and imidazo[1,2-*b*]pyridazine^[25] (Figure 2). In our continued efforts to develop alternate classes of p38 MAP kinase inhibitors, we designed and reported the imidazo[4,5-*b*]pyridin-2-one series^[26] of lead compounds with structures entirely different from those of the 1,3-thiazole series or the imidazo[1,2-*b*]pyridazine series. In addition to structural differentiation, as we reported in previous paper,^[26] the lead compound **1** can bind to Met109 and Gly110 in the peptide-flipped hinge region. It is supposed that the induction of the peptide-flipped hinge conformation contributes to high kinase selectivity.^[27] Lead compound **1** showed potent p38 MAP kinase inhibition (IC₅₀ = 9.6 nM) and suppressed the TNF- α -induced production of interleukin-8 (IL-8) in human whole blood (hWB) cell assay (IC₅₀ = 15 nM), as shown in Figure 3. However, its ability to suppress the lipopolysacchar-

[a] A. Kaieda, Dr. M. Takahashi, H. Fukuda, Dr. R. Okamoto, Dr. S. Morimoto, M. Gotoh, T. Miyazaki, Y. Hori, S. Unno, Dr. T. Kawamoto, Dr. T. Tanaka, Dr. S. Itono, T. Takagi, Dr. H. Sugimoto, Dr. K. Okada, Dr. S. Matsunaga, Dr. S. Miwatashi
Pharmaceutical Research Division
Takeda Pharmaceutical Company Limited
26-1, Muraoka-higashi 2-chome, Fujisawa, Kanagawa 251-8555 (Japan)
E-mail: akira.kaieda@takeda.com

[b] Dr. W. Lane, Dr. B.-C. Sang, Dr. K. Saikatendu
Takeda California
10410 Science Center Drive
San Diego, CA 92121 (USA)

Supporting information for this article is available on the WWW under <https://doi.org/10.1002/cmdc.201900373>

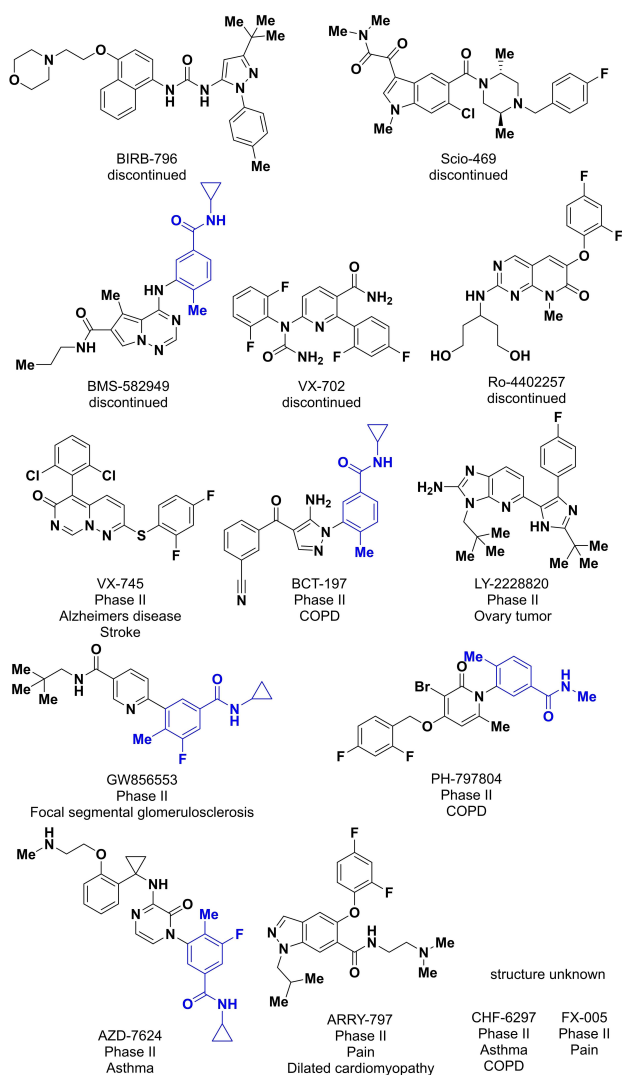


Figure 1. Representative p38 MAP kinase inhibitors.

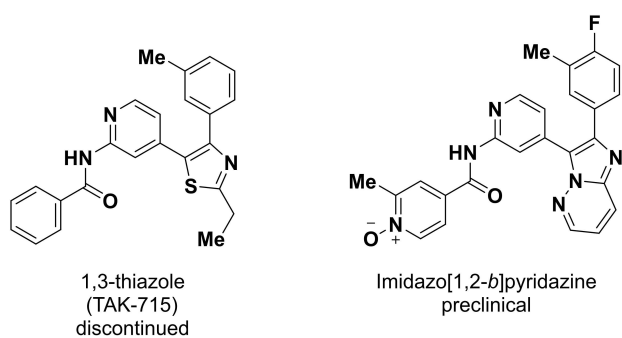
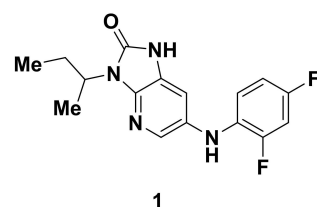


Figure 2. Structure of 1,3-thiazole and imidazo[1,2-b]pyridazine derivatives as p38 MAP kinase inhibitors.

ide (LPS)-induced production of TNF- α was found to be drastically attenuated in the hWB cell assay (IC_{50} = 2600 nM). We therefore hypothesized that a more potent enzymatic inhibition would be necessary for further enhancing cellular activity. In



1
p38 MAPK: IC_{50} = 9.6 nM
THP-1 (TNF- α): IC_{50} = 46 nM
hWB (IL-8): IC_{50} = 15 nM
hWB (TNF- α): IC_{50} = 2600 nM

Figure 3. Inhibitory activities of 1 on enzymatic and cellular activities.

order to validate this hypothesis, we proceeded to modify compound 1 by employing a structure-based design strategy. In order to confirm the increase in cellular activity, human monocytic leukemia cells (THP-1 cells) were used instead of hWB cells to evaluate the suppression in the LPS-induced production of TNF- α .

Imidazo[4,5-*b*]pyridin-2-one (2) was successfully co-crystallized with the ATP binding domain of p38 MAP kinase (Figure 4 upper part).^[26] Using information from the three-dimensional structure of the protein-ligand complex, we employed an expanding approach by targeting some of the interactions of the ligand with the back pocket of the enzyme for generating a novel p38 MAP kinase inhibitor scaffold. A research group at Eberhard-Karls-University Tubingen previously reported this approach to enhance enzymatic inhibitory activity of dibenzepinone-based p38 MAP kinase inhibitors.^[28] As highlighted in Figure 1, the structures of BMS-582949,^[29] BCT-197, GW856553, PH-797804, and AZD-7624 share common fragments, including

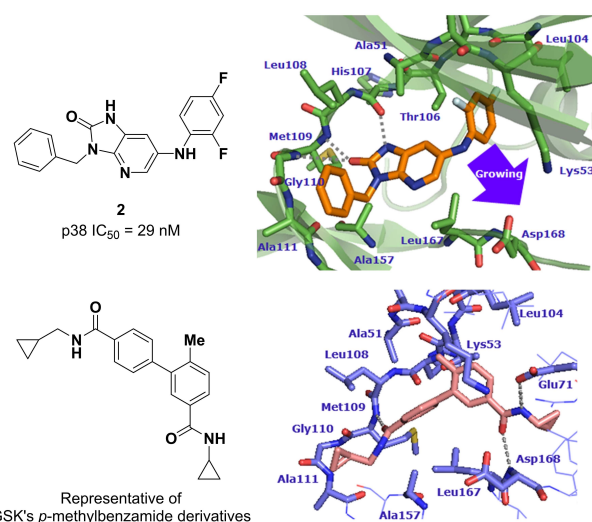


Figure 4. Structure of 2 (upper left) and X-ray crystal structure of the complex of 2 and the p38 MAP kinase (upper right; PDB code 6M9L). The purple arrow shows the direction of formation of direct hydrogen bonding with the enzyme back pocket residues. Structure (lower left) and X-ray crystal structure of the complex (lower right) of a representative of GSK's *p*-methylbenzamide derivatives.

the *p*-methylbenzamide moiety, which frequently binds to the back pocket of p38 MAP kinase. Using X-ray crystallography, a group of researchers at GSK demonstrated that the amide group of the methylbenzamide moiety of biphenyl amide derivatives has hydrogen bonding interactions with Glu71 and Asp168 in the back pocket of the enzyme (Figure 4 lower part).^[30,31] Based on the information on the binding properties of compound 2 combined with the data on the biphenyl amide derivatives developed by GSK, we designed and synthesized hybrid compounds from compound 1 that could interact directly with the back pocket of p38 MAP kinase (Figure 5). Herein, we report imidazo[4,5-*b*]pyridin-2-one core was successfully linked with the *p*-methylbenzamide fragment. We subsequently discovered compound 25, through structure activity relationship (SAR) studies and optimization, which exhibited exceptional enzymatic inhibition ($IC_{50} = 0.42$ nM), potent cellular activity, and significant dose-dependent *in vivo* efficacy in rats. Lead optimization, including the design, synthesis, and evaluation of the biological activity of imidazo[4,5-*b*]pyridin-2-one derivatives are also discussed herein for advancing the development of p38 MAP kinase inhibitors with variable scaffolds.

Results and Discussion

We recently reported the imidazo[4,5-*b*]pyridin-2-one derivative, compound 1, which exhibited potent p38 MAP kinase inhibition

activity (9.6 nM), as shown in Figure 3. However, since the suppression of the LPS-induced production of TNF- α in the hWB cell assay by compound 1 was relatively poor ($IC_{50} = 2600$ nM), we hypothesized that a further increase in the enzymatic activity would enhance cellular activity. Co-crystallization study of the analogous compound 2 with the ATP binding site of p38 MAP kinase (Figure 4 upper right)^[26] revealed that the NH group of aniline interacts with the protein back pocket site, via water-mediated hydrogen bonds with Lys53 and Asp168. In contrast, X-ray crystallography of *p*-methylbenzamide derivatives complexed with p38 MAP kinase revealed that the amide moiety directly interacts with Glu71 and Asp168 in the enzyme back pocket via hydrogen bonds (Figure 4 lower right).^[30] Based on the information from the co-crystallization studies of compound 2 and the methylbenzamide derivatives, we designed and synthesized the hybrid compounds from compound 1, that would directly interact with the back pocket of p38 MAP kinase (Figure 5).

The inhibitory properties, measured by the IC_{50} values, of the synthesized compounds were evaluated by using the p38 MAP kinase assay. Human monocytic leukemia cells (THP-1 cells) were used to assess the effects of the p38 MAP kinase inhibitors on cytokine production. As expected, the p38 MAP kinase inhibitory activity of the biaryl derivative, compound 3, dramatically increased by more than 10-fold in comparison with that of the lead compound 1, with the IC_{50} value being 0.73 nM (Table 1). Furthermore, the suppression in TNF- α production

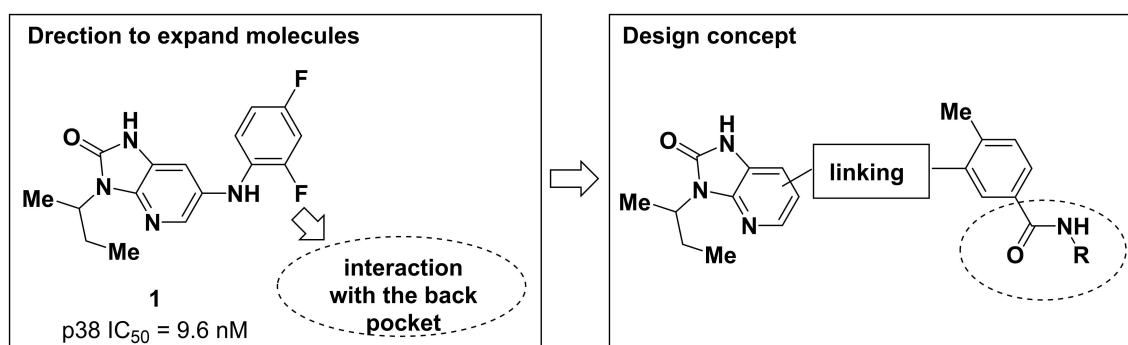


Figure 5. Expanding approach for direct hydrogen bond formation with the back pocket residues of the p38, and the design concept using *p*-methylbenzamide moiety.

Table 1. Inhibitory activities of imidazo[4,5-*b*]pyridin-2-one derivatives 3–6 against the p38 MAP kinase and production of TNF- α in human THP-1 cells.

ID	Position	X	p38 $IC_{50}^{[a]}$ (nM)	THP-1 $IC_{50}^{[a]}$ (nM)
3	6	bond	0.73 (0.68–0.78)	7.7 (4.6–13)
4	6	NH	41 (36–46)	370 (160–840)
5	7	bond	82 ^[b]	ND ^[c]
6	7	NH	3.5 (3.2–3.8)	65 (34–130)

[a] The IC_{50} values shown are the mean values of quadruple measurements; the numbers in parentheses represent the 95% confidence intervals. [b] The IC_{50} value shown is the value of single measurements [c] No data.

($IC_{50} = 7.7$ nM) by the biaryl compound **3** was higher in THP-1 cells than that induced by compound **1**. In order to obtain the SAR of compound **3**, we synthesized and evaluated compounds **4–6** with modified linkers and observed that the inhibitory activity of the biaryl compound **3** against p38 MAP kinase and the production of TNF- α in THP-1 cells were the highest among these compounds. Based on these results, we proceeded to optimize the benzamide moiety of compound **3**.

As indicated in Table 2, the *m*-methyl compound **7** exhibited an approximate 600-fold decrease in inhibitory activity, in comparison to that of compound **3**. The *o*-methyl group of compound **3** was found to be important for p38 MAP kinase inhibition. The *o*-methyl group induced a torsion between the imidazo[4,5-*b*]pyridin-2-one ring and the phenyl ring, and this torsion was considered to be sufficient to induce the benzamide moiety to interact with the back pocket of the enzyme. Furthermore, since the *p*-amide compound **8** also showed no inhibitory activity up to a concentration of 10 μ M, it was concluded that the orientation of substituents on the phenyl group of compound **3** was essential for the inhibitory activity. In order to confirm the effect of the *o*-methyl group on the phenyl group, the methyl group was substituted by a chloro

(**9**), fluoro (**10**), ethyl (**11**), and cyano (**12**) group. Compound **9**, bearing the chloro substituent, retained the inhibitory activity against p38, whereas compounds **10**, **11**, and **12**, bearing the fluoro, ethyl, and cyano substituents exhibited moderate but weaker inhibitory potencies than compound **3**, which bore the methyl substituent. These results further confirmed that the presence of a methyl substituent at the ortho position positively contributed to a strong inhibitory activity. It could be further inferred that the strength of the inhibitory activity against p38 MAP kinase was affected by the size of the ortho substituent and not by its electrostatic effect, since the bulkiness of the methyl or chloro group adequately corresponded to the space between the enzyme and the ligand. The replacement of the phenyl group in compound **3** by a thiophen group (**13**), which is a bioisostere of phenyl group, reduced the inhibitory activity. The reason behind the decrease in the inhibitory activity of compound **13** could be attributed to the fact that the S–O interaction between the sulfur of thiophen and the oxygen of the carbonyl group altered the direction of the amide bond in an unfavorable manner.

The effects of the substituent on the inhibitory activities of the compounds are depicted in Table 3. Our previous study

Table 2. The inhibitory activities of imidazo[4,5-*b*]pyridin-2-one derivatives **7–13** against the p38 MAP kinase.

ID	R ¹	R ²	R ³	R ⁴	IC ₅₀ ^[a] (nM)
3	Me	H	H	CONH ^t Pr	0.73
7	H	Me	H	CONH ^t Pr	440 (390–500)
8	Me	H	CONH ^c Pr	H	> 10000
9	Cl	H	H	CONH ^t Pr	0.79 (0.72–0.87)
10	F	H	H	CONH ^t Pr	16 (15–18)
11	Et	H	H	CONH ^t Pr	11 (9.6–12)
12	CN	H	H	CONH ^t Pr	17 (15–19)
13	NA ^[b]	NA ^[b]	NA ^[b]	NA ^[b]	1300 (1200–1500)

[a] The IC₅₀ values shown are the mean values of quadruple measurements; the numbers in parentheses represent the 95% confidence intervals. [b] Not applicable.

Table 3. The inhibitory activities of imidazo[4,5-*b*]pyridin-2-one derivatives **14–21** against the p38 MAP kinase.

ID	R ¹	IC ₅₀ ^[a] (nM)	ID	R ¹	IC ₅₀ ^[a] (nM)
14	3-Pen	0.79 (0.74–0.86)	18	C(Me) ₂ CH ₂ OH	1.1 (1.0–1.3)
15	^t Bu	0.77 (0.72–0.83)	19	4-pyranyl	2.1 (1.9–2.2)
16	^t Bu	1.3 (1.2–1.4)	20	1-Me- ^c Pr	1.4 (1.3–1.6)
17	CH ₂ ^c Pr	1.8 (1.6–2.0)	21	1-Me-oxetanyl	5.1 (4.4–5.9)

[a] The IC₅₀ values shown are the mean values of quadruple measurements; the numbers in parentheses represent the 95% confidence intervals.

demonstrated that the R¹ substituent on the nitrogen atom of imidazo[4,5-*b*]pyridin-2-one is important since it influences not only the inhibitory activity of the compound, but also its water solubility.^[26] We further identified that branched alkyls such as secondary butyl or 3-pentyl groups increases the inhibitory activity of the compound and its water solubility, making them more preferable substituents. We therefore focused on using branched R¹ substituents in this study. The inhibitory activities of compounds **14** and **15**, bearing 3-pentyl and tertiary butyl substituents, respectively, were comparable to that of compound **3**, bearing a secondary butyl substituent, whereas the inhibitory activities of compounds **16** and **17**, carrying isobutyl and cyclopropylmethyl substituents, respectively, were slightly reduced in comparison to that of compound **3**. These results were consistent with those of our previous study, in which the presence of a alkyl group branched at the alpha-carbon adjacent to the nitrogen atom on imidazo[4,5-*b*]pyridin-2-one conferred a strong p38 MAP kinase inhibitory activity.^[26] It should also be noted that an achiral substituent such as the 3-pentyl group of compound **14** or the tertiary butyl group of compound **15** facilitates the optimization process compared to the racemate secondary butyl substituent of compound **3**. The addition of a hydroxyl group (**18**) to the tertiary butyl group slightly decreased its inhibitory activity. Substitutions with 4-pyranyl, 1-methylcyclopropyl, and 1-methyloxetanyl groups in compounds **19**, **20**, and **21**, respectively, also decreased their inhibitory activity.

We then proceeded to optimize the amide side chain of the benzamide moiety of compound **15**. Substitutions with alkyl groups, namely, methyl, cyclobutyl, or isopropyl groups in compounds **22**, **23**, and **24**, respectively, decreased their inhibitory potential. The observation that compound **15**, with the cyclopropyl substituent, was more potent than compound **24**, bearing the isopropyl substituent, led us to the idea that sp² character of cyclopropane ring could play an important role in enhancing the p38 MAP kinase inhibitory activity. It was previously reported by a research group at BMS that the p38 MAP kinase inhibitory activity is retained upon substitution of the amide side chain by an azole group.^[32] The effect of

replacing the cyclopropyl group with an azole group on the inhibitory activity was explored. It was observed that substitution with 4-isoxazolyl **26** decreased the inhibitory activity; however, substitution with 3-isoxazolyl **25**, pyrazolyls **27–28** and 5-thiazol **29** retained their potent p38 MAP kinase inhibitory activity. Compound **25**, with the 3-isoxazolyl substituent, exhibited the most potent inhibition, with an IC₅₀ value of 0.42 nM, and was successfully co-crystallized with the ATP binding domain of p38 MAP kinase at a resolution of 2.5 Å (Figure 6). The X-ray structure of the complex of compound **25** with the enzyme revealed that compound **25** binds to the enzyme as expected, and the flipped amide bond between Met109 and Gly110 was also observed.^[26] The carbonyl oxygen and the 3-NH hydrogen of the imidazo[4,5-*b*]pyridin-2-one ring interact with the hinge region via hydrogen bonds with Gly110, Met109, and His107 (Figure 6, Left). The carbonyl oxygen and the N–H group of the benzamide moiety form direct hydrogen bonding interactions with Asp168 and Glu71, respectively. In addition to these electrostatic interactions, the terminal isoxazole ring stacks perpendicularly with Phe169 of DFG which adopts DFG-in conformation. These CH-π interactions of the azole groups, such as the R¹ group of compound **25** and compounds **27–29** contribute to the increase in their inhibitory activity, as shown by the SAR study (Table 4). Additionally, the methylbenzene group filled the inner shallow hydrophobic pocket of the p38 MAP kinase, comprising Thr106 and Leu104. The imidazo[4,5-*b*]pyridin-2-one ring was found to be sandwiched between Ala51/Val38 of the N-lobe and Leu167 of the C-lobe (Figure 6, Right). Compound **25** exhibited excellent selectivity among the 28 kinases in a kinase panel study aimed to probe the potential off-target liabilities (Table S1). It is also worth to note that compound **25** exhibited excellent selectivity against the 312 kinases in the TR-FRET based competitive binding assay (Kinome MAP (Figure S1) are provided in the supporting information).^[33] Compound **25** showed the inhibitory activities against BRAF, LYN, RET, p38δ (6 < pIC₅₀ < 7), RIPK2 (7 < pIC₅₀ < 8), p38α, p38β, p38γ (pIC₅₀ > 8).

The potential of the p38 MAP kinase inhibitors were evaluated by hWB cell-based assays.^[27] Owing to the relative

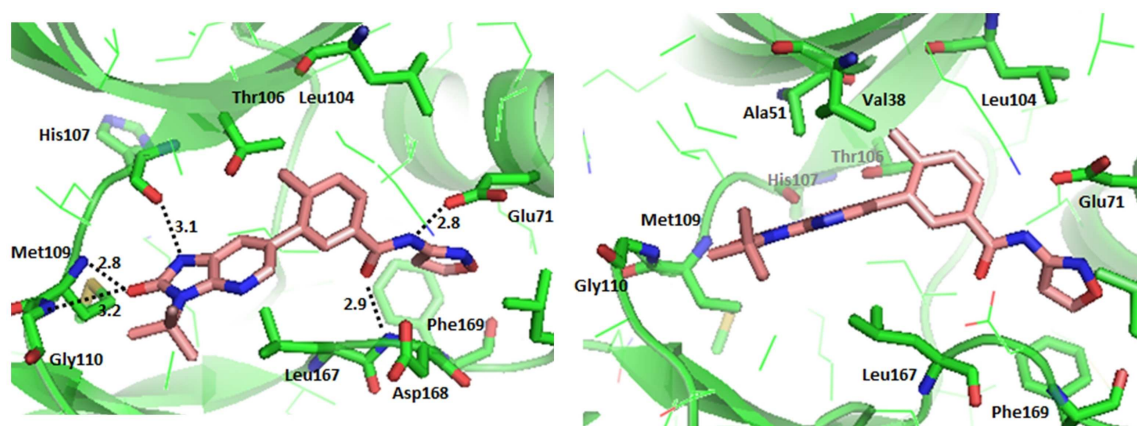
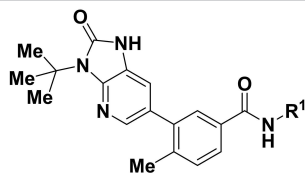


Figure 6. X-ray crystal structure of the complex of **25** and the p38 MAP kinase (PDB code 6OHD). Left: top view, Right: side view.

Table 4. The inhibitory activities of imidazo[4,5-*b*]pyridin-2-one derivatives **22–29** against the p38 MAP kinase.

ID	R ¹	IC ₅₀ ^[a] (nM)	ID	R ¹	IC ₅₀ ^[a] (nM)
22	Me	2.7 (2.2–3.3)	26	4-isoxazolyl	2.2 (1.9–2.5)
23	^t Bu	1.2 (1.1–1.4)	27	1-Me-3-pyrazolyl	0.86 (0.78–0.94)
24	ⁱ Pr	2.6 (2.2–3.0)	28	1-Me-5-pyrazolyl	0.78 (0.71–0.86)
25	3-isoxazolyl	0.42 (0.36–0.48)	29	5-thiazolyl	0.81 (0.72–0.91)

[a] The IC₅₀ values shown are the mean values of quadruple measurements; the numbers in parentheses represent the 95% confidence intervals.



complexity of the cell-based assay, the suppression of cytokine production in the hWB assay is considered to reflect the *in vivo* efficacy of the compound. The inhibitory potencies, measured in terms of the IC₅₀ values, of the representative compounds are summarized in Table 5. These compounds, namely, compounds **3**, **9**, **14**, **15**, **25**, **27**, **28**, and **29**, which exhibited highly potent p38 MAP kinase inhibition, inhibited the LPS-induced production of TNF- α in THP-1 cells with IC₅₀ values ranging between 0.49 and 18 nM. Interestingly, compounds **3**, **9**, and **14** exhibited more than 10-fold decrease between p38 inhibition and THP-1 cell-based inhibition, whereas the *tert*-butyl compounds, namely, compounds **15**, **25**, and **27–29** exhibited only a relatively slight decrease. Additionally, these compounds suppressed the TNF- α -induced production of IL-8 in hWB cells. Unlike the results of the THP-1 cell assay, compounds **3**, **14**, **15**, and **25** exhibited a strong suppression in IL-8 production. Compounds **15**, **25**, and **28** exhibited a potent inhibition of the LPS-induced production of TNF- α . The explanation on discrepancy in the inhibitory activity of the compounds between the two cell-based assays was still ambiguous, and it was also not

possible to explain the differences in the SAR of the compounds between the two cell-based assays. However, compounds **15** and **25** exhibited highly potent cytokine suppression in both the cell-based assays. The pharmacokinetic properties of compounds **15** and **25** in rats are shown in Table 6. It was observed that compound **25** exhibited a higher oral exposure (AUC = 370.4 ng h/mL) and bioavailability (*F*% = 41.6); however, compound **15** exhibited a lower oral exposure and bioavailability (AUC = 194.6 ng h/mL; *F*% = 20.7). At a dose of 1 mg/kg, the absorption and exposure of compound **25** were favorable in rats and were sufficient for further *in vivo* pharmacological testing.

Compound **25** was evaluated in a pseudoestablished rat model of collagen-induced arthritis (CIA) (Figure 7). The rats were orally administered compound **25**, with b.i.d. dosing, at doses of 0.1, 0.3, and 1 mg/kg for 2 days. The swelling of the paws was measured on day 14. Compound **25** exhibited dose-dependent efficacy in markedly reducing paw swelling at doses of 0.1–1.0 mg/kg. At doses of 0.1, 0.3, and 1.0 mg/kg, the

Table 5. The inhibitory activities of imidazo[4,5-*b*]pyridin-2-one derivatives **3**, **9**, **14**, **15**, **25**, and **27–29** on TNF- α production in human THP-1 cells, and IL-8 production and TNF- α production in human whole blood cells.

ID	p38 MAPK IC ₅₀ ^[a] (nM)	THP-1 IC ₅₀ ^[a] (nM)	hWB IL-8 IC ₅₀ ^[a] (nM)	hWB TNF- α IC ₅₀ ^[a] (nM)	Solubility pH = 6.8 (μ g/mL)
3	0.73	7.7	2.4 (2.0–2.7)	170 (130–210)	6.5
9	0.79	18 (10–30)	8.1 (6.1–10)	450 (200–700)	3.1
14	0.79	9.4 (5.5–16)	2.6 (1.3–4.0)	150 (71–220)	2.0
15	0.77	1.4 (0.95–2.0)	2.0 (0.96–3.1)	61 (40–82)	3.6
25	0.42	0.49 (0.23–1.0)	2.5 (1.7–3.4)	30 (28–33)	5.5
27	0.86	1.5 (0.95–1.3)	7.4 (4.8–10)	150 (78–210)	3.2
28	0.78	1.4 (0.86–2.2)	7.1 (4.5–9.8)	70 (42–97)	49
29	0.81	3.1 (1.7–5.4)	93 (23–160)	510 (490–530)	0.76

[a] The IC₅₀ values shown are the mean values of more than double measurements; the numbers in parentheses represent the 95% confidence intervals.

Table 6. Pharmacokinetic parameters of **15** and **25** in rats^[a].

ID	C _{max} ^[b] (ng/mL)	T _{max} ^[b] (h)	AUC ^[b] (n-g h/mL)	MRT ^[b] (h)	V _d (mL/kg)	CL (mL/h/kg)	<i>F</i> (%)
15	55.2	1.0	194.6	2.5	2145	1067	20.7
25	98.5	1.3	370.4	2.5	1947	1169	41.6

[a] Mean values of measurements conducted in three animals; i.v. 0.1 mg/kg, p.o. 1.0 mg/kg in 0.5% methyl cellulose suspension. [b] p.o. data.

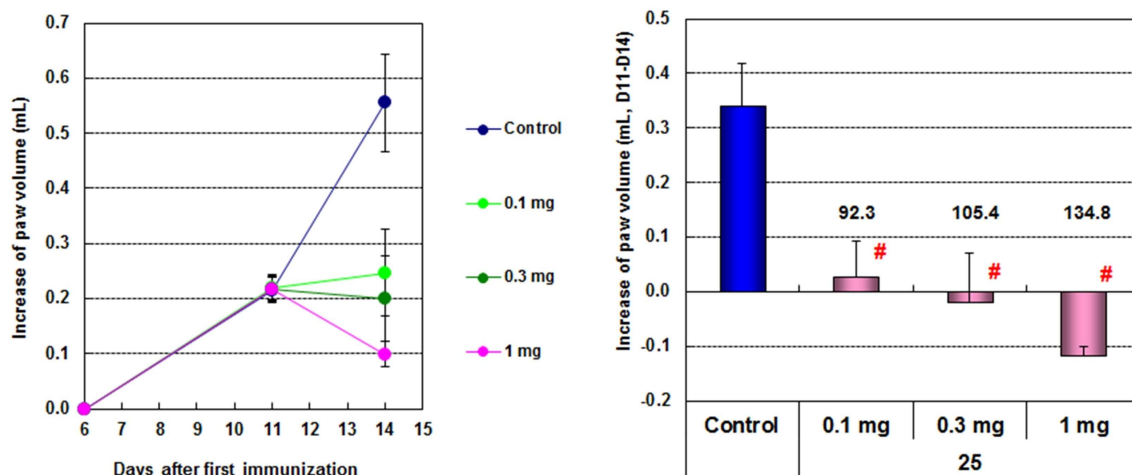
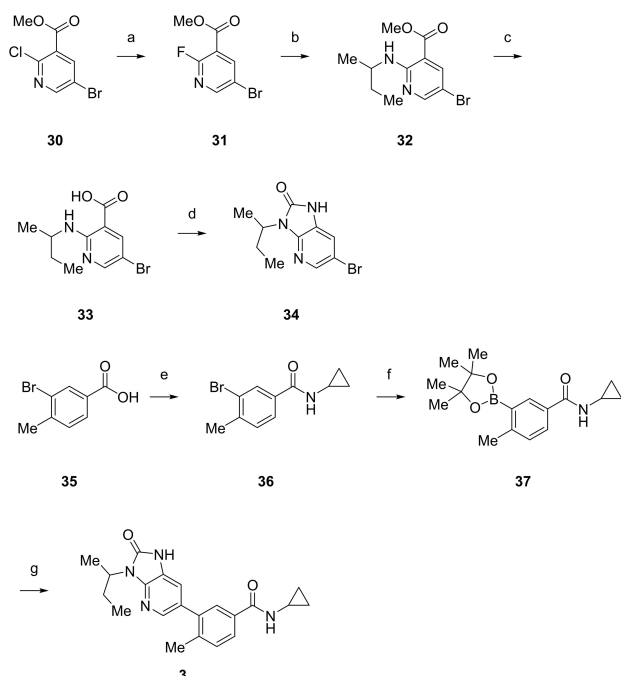


Figure 7. Anti-inflammatory effects of **25** in the model of collagen-induced arthritis in the rat (bid, po, 2 days treatment). Left: Time course; Right: paw volume at day 14. Data represent the mean \pm S.E. for 5 or 8 animals/group. #: $p < 0.025$ vs. control by Williams test.

reduction in paw swelling was found to be statistically significant.

Chemistry

The synthesis route of compound **3** is indicated in Scheme 1 as a representative route for the synthesis of imidazo[4,5-*b*]pyridin-2-one analogs (experimental procedures for compounds



Scheme 1. Synthesis of compounds **3**. Reagents and conditions: (a) CsF, DMSO, 50 °C; (b) 1-methylpropylamine, DMSO, 100 °C; (c) 8 N NaOH, THF-MeOH, rt; (d) DPPA, Et₃N, toluene, 100 °C; (e) cyclopropylamine, WSC, HOBT, Et₃N, DMF rt; (f) (Bpin)₂, PdCl₂(dppf)·CH₂Cl₂, NaOAc, DME, reflux; (g) PdCl₂(dppf)·CH₂Cl₂, Na₂CO₃, DME-H₂O, 100 °C.

3–29 and intermediates are provided in the supporting information). In Scheme 1, chloropyridine **30** was treated with cesium fluoride to afford fluoropyridine **31**.^[26] An aromatic nucleophilic substitution reaction with the appropriate amines R¹NH₂ produced the corresponding compound **32**. The alkaline hydrolysis of **32** produced the carboxylic acid **33** as a cyclization precursor. Subsequent cyclization was successfully accomplished by treating compound **33** with DPPA. Amidation of the carboxylic acid **35** and subsequent Miyaura-borylation of **36** led to the generation of compound **37**. The Suzuki-Miyaura cross coupling reaction of compounds **34** and **37** finally led to the generation of compound **3**.

Conclusions

In our structure-based design strategy beginning from lead compound **1**, we focused on the design and synthesis of hybrid compounds in which the imidazo[4,5-*b*]pyridin-2-one core was successfully linked with the *p*-methylbenzamide fragment, to enhance the suppression of the LPS-induced production of TNF- α in the hWB cell assay. The SAR analyses revealed that compound **25** had excellent p38 MAP kinase inhibitory activity (IC₅₀ = 0.42 nM), suppressed the production of TNF- α in hWB cells (IC₅₀ = 30 nM), and had good oral bioavailability in rats. It was further observed that compound **25** exhibited dose-dependent efficacy in a rat model of CIA at doses between 0.1–1.0 mg/kg.

Experimental Section

Biology: p38 MAP kinase enzyme assay.^[25,26] According to previously reported method, the FLAG-tagged human p38- α protein was expressed, activated, and purified. Kinase reactions were evaluated with LanthaScreen assay system; 2.5 μ L of test compounds, diluted with DMSO (final concentration 1% DMSO), were added to the reaction mixture (25 mM HEPES [pH 7.5], 10 mM

Mg acetate, 1 mM DTT, 0.01% Tween-20, and 0.01% BSA) containing 125 pg human p38- α protein and 8 nM GFP-ATF2. After a 5 min incubation at room temperature, 5 μ L of 580 μ M ATP was added to the reaction mixture. After a 20 min incubation, 5 μ L of 80 mM EDTA was added to the reaction mixture. Then, 5 μ L of the Tb-anti-phospho ATF2 (pThr71) antibody (Life Technologies) was added and subsequently incubated for 60 min at room temperature. The time-resolved fluorescence resonance energy transfer (TR-FRET) signal was measured using EnVision Multilabel Plate Reader (PerkinElmer).

TNF- α production assay in THP-1 cells.^[25,26] THP-1 cells were suspended in RPMI 1640 medium (Life Technologies) containing 1% fetal bovine serum (Morgate, Australia) according to previously reported method. Then, 40 μ L of the cell suspension (0.625×10^6 cells/mL) was incubated with 5 μ L of test compounds diluted with 10% DMSO. After 60 min incubation at 37 °C under 5% CO₂, the cells were activated with 5 μ L of 100 μ g/mL LPS (Wako). After incubating for 4 h at 37 °C under 5% CO₂, the concentration of TNF- α in the medium was measured with the TNF- α HTRF kit (CisBio, USA). The TR-FRET signal was detected with EnVision Multilabel Plate Reader.

IL-8 or TNF- α production assay in human whole blood cells.^[26] Human whole blood was diluted with RPMI 1640 medium (Nikken-bio) to be 2.5 times. Then, 160 μ L of the diluted blood was added to 96-well plates and mixed with 20 μ L of test compounds diluted with 10% DMSO. After 60 min incubation at 37 °C and 5% CO₂, the blood was stimulated with 20 μ L of 300 ng/mL human TNF- α or 20 μ L of 10 ng/mL LPS. After incubating for 18–24 h at 37 °C and 5% CO₂, the concentration of IL-8 or TNF- α in the medium was measured with the IL-8 or TNF- α ELISA kit (R&D systems, USA). The absorbance was measured with Wallac 1420 Plate Reader (PerkinElmer).

Solubility:^[25,26] According to the standard screening method in Takeda Pharmaceutical Company Limited, small volumes of the compound solution dissolved in DMSO were added to the aqueous buffer solution (pH 6.8). After incubation, precipitates were separated by filtration. The solubility was determined by HPLC analysis of each filtrate.

Pharmacokinetics: Rat cassette BA.^[26] According to the standard method in Takeda Pharmaceutical Company Limited, the compounds were administered intravenously (0.1 mg/kg) or orally (1 mg/kg) by cassette dosing to non-fasted rats. After administration, blood samples were collected and centrifuged to obtain the plasma fraction. The obtained plasma samples were deproteinized by mixing with acetonitrile followed by centrifugation. The compound concentrations in the supernatant were measured by LC-MS/MS. All the experiments using animals were reviewed and approved by the Internal Animal Care and Use Committee of Takeda Pharmaceutical Research Division.

Rat collagen model of induced arthritis.^[25] Rat CIA was induced according to previously reported method. On day 6 and 11, the volumes of both hind paws were measured using a Plethysmometer (UGO BASIL, Varese, Italy). The CIA rats were divided based on body weight and increase in paw volume ($n=8$ per group) on day 11: one group received 0.5% methyl cellulose (MC), while the other five groups received compounds suspended in 0.5% MC at a dosage of 0.1–1 mg/kg. The increase in paw volume was expressed as the value of paw volume measured on day 11, minus the value of the paw volume measured on day 6, in each CIA rat. The compounds were administered to rats twice a day from day 12 to day 13. The same paw was subsequently measured on day 14. Differences between the means of the control and drug-treated groups were analyzed using the Williams test. All the experiments

using animals were reviewed and approved by the Internal Animal Care and Use Committee of Takeda Pharmaceutical Research Division.

Author Contributions

The manuscript was written through contributions of all authors. All authors have given approval to the final version of the manuscript. A. K., M. T., H. F., R. O., S. M., S. M. and S. M. contributed design and synthesis of compounds; M. G., T. M., Y. H., S. U., T. K., and H. S. conducted in vitro and in vivo study; T. T., S. I., T. T., K. O., W. L., B. S. and K. S. contributed x-ray crystallography.

Abbreviations

MAP	mitogen-activated protein
TNF- α	tumor necrosis factor- α
IL-1 β	interleukin-1 β
IL-8	interleukin-8
RA	rheumatoid arthritis
LPS	lipopolysaccharide
hWB	human whole blood
CIA	collagen-induced arthritis
SAR	structure-activity relationships

Acknowledgements

The authors express their gratitude to Drs. Shigenori Ohkawa, Yuji Ishihara, Fumio Itoh, Osamu Uchikawa, and Yoshinori Ikeura for their valuable discussions, and to Dr. Takashi Ichikawa for critically reviewing the manuscript. The authors remain grateful to the members of the Takeda Analytical Research Laboratories, Ltd., for performing the elemental analyses. We thank the staff at Berkeley Center for Structural Biology, Lawrence Berkeley National Laboratory, wherefrom the X-ray diffraction data were collected using the Advanced Light Source beamline 5.0.3. The Berkeley Center for Structural Biology is supported in part by the National Institutes of Health, National Institute of General Medical Sciences, and the Howard Hughes Medical Institute. The Advanced Light Source is a Department of Energy Office of Science user facility under contract no. DE-AC02-05CH11231.

Conflict of Interest

The authors declare no conflict of interest.

Keywords: p38 mitogen-activated protein kinase inhibitors · rheumatoid arthritis · structure-based design · imidazo[4,5-*b*]pyridin-2-one derivatives

[1] G. Schett, J. Zwerina, G. Firestein, *Ann. Rheum. Dis.* **2008**, *67*, 909–916.

[2] J. Westra, C. P. Limburg, *Mini-Rev. Med. Chem.* **2006**, *6*, 867–874.

- [3] G. Schett, C. Stach, J. Zwerina, R. Voll, B. Manger, *Arthritis Rheum.* **2008**, *58*, 2936–2948.
- [4] V. Strand, A. J. Singh, *Am. J. Manag. Care* **2008**, *14*, 234–254.
- [5] J. M. Elliott, M. N. Cerami, M. Feldmann, R. J. Kalden, C. Antoni, S. J. Smolen, B. Leeb, C. F. Breedveld, D. J. Macfarlane, H. Bijl, N. J. Woody, *Lancet* **1994**, *344*, 1105–1110.
- [6] C. C. Rankin, S. E. H. Choy, D. Kassimos, H. G. Kingsley, M. A. Sopwith, A. D. Isenberg, S. G. Panayi, *Br. J. Rheumatol.* **1995**, *34*, 334–342.
- [7] M. H. Van Dulleman, J. S. Van Deventers, W. D. Hommens, H. Bijl, J. Jansen, N. J. Woody, *Gastroenterology* **1995**, *109*, 129–135.
- [8] T. Patel, B. K. Gordon, *Dermatol Ther.* **2004**, *17*, 427–431.
- [9] M. L. Bang, M. G. Keating, *BioDrugs* **2004**, *18*, 121–139.
- [10] W. L. Moreland, W. S. Baumgartner, H. M. Schiff, A. E. Tindall, M. R. Fleischmann, L. A. Weaver, E. R. Ettliger, S. Cohen, J. W. Koopman, K. Mohler, B. M. Widmer, M. C. Bloesch, *N. Engl. J. Med.* **1997**, *337*, 141–147.
- [11] K. K. Hale, D. Trollinger, M. Rihaneck, L. C. Manthey, *J. Immunol.* **1999**, *162*, 4246–4252.
- [12] A. Korb, M. Tohidast-Akrad, E. Cetin, R. Axmann, J. Smolen, G. Schett, *Arthritis Rheum.* **2006**, *54*, 2745–2756.
- [13] G. Schett, M. Tohidast-Akrad, S. J. Smolen, J. B. Schmid, W. C. Steiner, P. Bitzan, P. Zenz, K. Redlich, Q. Xu, G. Steiner, *Arthritis Rheum.* **2000**, *43*, 2501–2512.
- [14] M. D. Goldstein, T. Gabriel, *Curr. Top. Med. Chem.* **2005**, *5*, 1017–1029.
- [15] H. L. Pettus, P. R. Wurz, *Curr. Top. Med. Chem.* **2008**, *8*, 1452–1467.
- [16] S. Miwatashi, Y. Arikawa, E. Kotani, M. Miyamoto, K. Naruo, H. Kimura, T. Tanaka, S. Asahi, S. Ohkawa, *J. Med. Chem.* **2005**, *48*, 5966–5979.
- [17] G. Zlokarnik, J. P. D. Grootenhuys, B. J. Watson, *Drug Discovery Today* **2005**, *10*, 1443–1450.
- [18] A. T. Halgren, *J. Comput. Chem.* **1999**, *20*, 720–729.
- [19] M. D. Goldstein, A. Kuglstatler, Y. Lou, J. M. Soth, *J. Med. Chem.* **2010**, *53*, 2345–2353.
- [20] P. J. Duffy, M. E. Harrington, G. F. Salituro, E. J. Cochran, J. Green, H. Gao, W. G. Bemis, G. Evindar, P. V. Galullo, J. P. Ford, A. U. Germann, P. K. Wilson, F. S. Bellon, G. Chen, P. Taslimi, P. Jones, C. Huang, S. Pazhanisamy, M. Y. Wang, A. M. Murcko, S. M. Su, *ACS Med. Chem. Lett.* **2011**, *2*, 758–63.
- [21] A. D. Lomas, A. D. Lipson, E. B. Miller, L. Willits, O. Keene, H. Barnacle, C. N. Barnes, R. Tal-Singer, *J. Clin. Pharmacol.* **2012**, *52*, 416–424.
- [22] H. Watz, H. Barnacle, F. B. Hartley, R. Chan, *Lancet Respir. Med.* **2014**, *2*, 63–72.
- [23] See [ClinicalTrials.gov](https://www.clinicaltrials.gov) (<https://www.clinicaltrials.gov/ct2/home>) to check the latest clinical information.
- [24] W. Albrecht, A. Unger, M. S. Bauer, A. S. Laufer, *J. Med. Chem.* **2017**, *60*, 5290–5305.
- [25] A. Kaieda, M. Takahashi, T. Takai, M. Goto, T. Miyazaki, Y. Hori, S. Unno, T. Kawamoto, T. Tanaka, S. Itono, T. Takagi, T. Hamada, M. Shirasaki, K. Okada, G. Snell, K. Bragstad, B. C. Sang, O. Uchikawa, S. Miwatashi, *Bioorg. Med. Chem.* **2018**, *26*, 647–660.
- [26] A. Kaieda, M. Takahashi, H. Fukuda, R. Okamoto, S. Morimoto, M. Gotoh, T. Miyazaki, Y. Hori, S. Unno, T. Kawamoto, T. Tanaka, S. Itono, T. Takagi, H. Sugimoto, K. Okada, G. Snell, R. Bertsch, J. Nguyen, B. C. Sang, S. Miwatashi, *ChemMedChem*, **2019**, *14*, 1022–1030.
- [27] C. S. Koeberle, J. Romir, S. Fischer, A. Koeberle, V. Schattel, W. Albrecht, C. Grutter, O. Werz, D. Rauh, T. Stehle, A. S. Laufer, *Nat. Chem. Biol.* **2012**, *8*, 141–143.
- [28] E. K. Martz, A. Dorn, B. Baur, V. Schattel, I. M. Goettert, C. S. Mayer-Wrangowski, D. Rauh, A. S. Laufer, *J. Med. Chem.* **2012**, *55*, 7862–7874.
- [29] C. Liu, J. Lin, T. S. Wroblewski, S. Lin, J. Hynes, H. Wu, J. A. Dyckman, T. Li, J. Wityak, M. K. Gillooly, S. Pitt, R. D. Shen, F. R. Zhang, W. K. McIntyre, L. Salter-Cid, J. D. Shuster, H. Zhang, H. P. Marathe, M. A. Doweiko, S. J. Sack, E. S. Kiefer, F. K. Kish, A. J. Newitt, M. McKinnon, H. J. Dodd, C. J. Barrish, L. G. Schieven, K. Leftheris, *J. Med. Chem.* **2010**, *53*, 6629–6639.
- [30] R. Angell, M. N. Aston, P. Bamborough, B. J. Buckton, S. Cockerill, J. S. de Boeck, D. C. Edwards, S. D. Holmes, L. K. Jones, I. D. Laine, S. Patel, A. P. Smee, J. K. Smith, O. D. Somers, L. A. Walker, *Bioorg. Med. Chem. Lett.* **2008**, *18*, 4428–4432.
- [31] M. N. Aston, P. Bamborough, B. J. Buckton, D. C. Edwards, S. D. Holmes, L. K. Jones, K. V. Patel, A. P. Smee, O. D. Somers, G. Vitulli, L. A. Walker, *J. Med. Chem.* **2009**, *52*, 6257–6269.
- [32] J. J. Hynes, H. Wu, S. Pitt, R. D. Shen, R. Zhang, L. G. Schieven, M. K. Gillooly, J. D. Shuster, L. T. Taylor, X. Yang, W. K. McIntyre, M. McKinnon, H. Zhang, H. P. Marathe, M. A. Doweiko, K. Kish, E. S. Kiefer, S. J. Sack, A. J. Newitt, C. J. Barrish, J. Dodd, K. Leftheris, *Bioorg. Med. Chem. Lett.* **2008**, *18*, 1762–1767.
- [33] Y. Hirozane, M. Toyofuku, T. Yogo, Y. Tanaka, T. Sameshima, I. Miyashita, M. Yoshikawa, *Bioorg. Med. Chem. Lett.* **2019**, in press.

Manuscript received: June 21, 2019
 Revised manuscript received: October 11, 2019
 Version of record online: ■■■, ■■■■

